



# 1 A percentile approach to evaluate simulated groundwater levels and 2 frequencies in a Chalk catchment in Southwest England

3 Simon Brenner<sup>1</sup>, Gemma Coxon<sup>2,4</sup>, Nicholas J. K. Howden<sup>3,4</sup>, J. Freer<sup>2,4</sup> and Andreas Hartmann<sup>1,3</sup>

4 <sup>1</sup>Institute of Earth and Environmental Sciences, Freiburg University, Germany

5 <sup>2</sup>School of Geographical Sciences, University of Bristol, Bristol, UK

6 <sup>3</sup>Department of Civil Engineering, University of Bristol, Bristol, UK

7 <sup>4</sup>Cabot Institute, University of Bristol, Bristol, UK.

8 *Correspondence to:* S. Brenner (simon.brenner@hydrology.uni-freiburg.de)

## 9 **Abstract.**

10 Chalk aquifers are an important source of drinking water in the UK. Understanding and predicting groundwater levels is therefore  
11 important for effective water management of this resource. Chalk is known for its high porosity and, due to its dissolvability, exposed  
12 to karstification and strong subsurface heterogeneity. To cope with the karstic heterogeneity and limited data availability, specialised  
13 modelling approaches are required that balance model complexity and data availability. In this study we present a novel approach  
14 to simulate groundwater level frequency distributions with a semi-distributed karst model that represents subsurface heterogeneity  
15 by distribution functions. Simulated groundwater storages are transferred into groundwater levels using evidence from different  
16 observations wells. Using a newly developed percentile approach we can simulate the number of days exceeding or falling below  
17 selected groundwater level percentiles. Firstly, we evaluate the performance of the model to simulate three groundwater time series  
18 by a split sample test and parameter identifiability analysis. Secondly, we apply a split sample test on the simulated groundwater  
19 level percentiles to explore the performance in predicting groundwater level exceedances. We show that the model provides robust  
20 simulations of discharge and groundwater levels at 3 observation wells at a test site in chalk dominated catchment in Southwest  
21 England. The second split sample test also indicates that percentile approach is able to reliably predict groundwater level  
22 exceedances across all considered time scales up to their 75th percentile. However, when looking at the 90th percentile, it only  
23 provides acceptable predictions for the longest available time scale and it fails when the 95th percentile of groundwater exceedance  
24 levels is considered. Modifying the historic forcings of our model according to expected future climate changes, we create simple  
25 climate scenarios and we show that the projected climate changes may lead to generally lower groundwater levels and a reduction  
26 of exceedances of high groundwater level percentiles.

## 27 **1 Introduction**

28 The English Chalk aquifer region extends over large parts of south-east England and is an important water resource aquifer,  
29 providing about 55 % of all groundwater-abstracted drinking water in the UK (Lloyd, 1993). As a carbonate rock the English Chalk  
30 is exposed to karstification, i.e. the chemical weathering (Ford and Williams, 2013), resulting in particular surface and subsurface  
31 features such as dolines, river sinks, caves and conduits (Goldscheider and Drew, 2007). Consequently, karstification also produces  
32 strong hydrological subsurface heterogeneity (Bakalowicz, 2005). The interplay between diffuse and concentrated infiltration and  
33 recharge processes, as well as fast flow through karstic conduits and diffuse matrix flow, result in complex flow and storage  
34 dynamics (Hartmann et al., 2014a). Even though Chalk tends to less intense karstification, for instance compared to limestone, its  
35 karstic behaviour has increasingly been recognised (Fitzpatrick, 2011; Maurice et al., 2006, 2012).

36 Apart from the good water quality, favourable infiltration and storage dynamics which make chalk aquifers a preferred source of  
37 drinking water in the UK, their karstic behaviour also increases the risk of fast drainage of their storages by karstic conduit flow  
38 during dry years. This also increases the risk of groundwater flooding as a result of fast responses of groundwater levels to intense



1 rainfalls due to fast infiltration and groundwater recharge processes. Groundwater flooding, i.e. when groundwater levels emerge at  
2 the ground surface due to intense rainfall (Macdonald et al., 2008), tend to be more severe in areas of permeable outcrop like the  
3 English Chalk (Macdonald et al., 2012). Groundwater drought indices tend to be more related to recharge conditions in Cretaceous  
4 Chalk aquifers than in granular aquifers (Bloomfield and Marchant, 2013). Due to the fast transfer of water from the soil surface to  
5 the main groundwater system, chalk aquifers tend to be more sensitive to external changes, for instance shown by Jackson et al.  
6 (2015) who found significant groundwater level declines in 4 out of 7 chalk boreholes in a UK-wide study using historic groundwater  
7 level observations.

8 Climate projections suggest that the UK will experience increasing temperatures, with less rainfall during the summer but warmer  
9 and wetter winters (Jenkins et al., 2008). This may stress these groundwater resources, and increase the risk of groundwater droughts  
10 and potentially winter groundwater flooding. For those reasons, assessment of potential future changes in groundwater dynamics,  
11 concerning groundwater droughts, median groundwater levels as well as groundwater flooding is broadly recommended (Jackson  
12 et al., 2015; Jimenez-Martinez et al., 2015). Physics based hydrological simulation models that incorporate hydrological processes  
13 in a relatively high detail can be considered to potentially provide the most reliable predictions, especially under a changing  
14 environment. However, there are considerable limitations in obtaining the necessary information to estimate the structure and the  
15 model parameters, especially for subsurface processes, and this inevitably increases modelling uncertainties (Beven, 2006; Perrin  
16 et al., 2003).

17 The definition of appropriate structures and parameters from limited information becomes problematic when modelling karst  
18 aquifers. In order to achieve acceptable simulation performance they have to include representations of karstic heterogeneity in their  
19 structures. Distributed karst modelling approaches are able simulate groundwater levels on a spatial grid but their data requirements  
20 mostly limit them to theoretical studies (e.g., Birk et al., 2006; Reimann et al., 2011) or well explored study sites (e.g., Hill et al.,  
21 2010; Jackson et al., 2011; Oehlmann et al., 2014). Lumped karst modelling approaches consider physical processes at the scale of  
22 the entire karst system. Although they are strongly simplified, they can include karst peculiarities such as different conduit and  
23 matrix systems (Fleury et al., 2009; Geyer et al., 2008; Maloszewski et al., 2002). Since they are easy to implement and don't require  
24 spatial information, they are widely used in karst modelling (Jukić and Denić-Jukić, 2009). Up to now, most lumped karst models  
25 have been applied for rainfall-runoff simulations. Groundwater levels were only simulated in some studies (Adams et al., 2010;  
26 Jimenez-Martinez et al., 2015; Ladouche et al., 2014), mostly relying on very simple representation of karst hydrological processes  
27 and disregarding the scale discrepancy between borehole (point scale) and modelling domain (catchment scale) at which they were  
28 applied.

29 In this study, we present a novel approach to simulate and predict groundwater level frequencies in chalk dominated catchments.  
30 This uses a previously developed semi-distributed process-based model (VarKarst, Hartmann et al., 2013b) that we further  
31 developed to simulate groundwater levels. To assess groundwater level frequencies we formulated a percentile of groundwater based  
32 approach that quantifies the probability of exceeding or falling below selected groundwater levels. We exemplify and evaluate our  
33 new approach on a Chalk catchment in Southwest England that had to cope with several flooding events in the past. Finally we  
34 apply the approach on simple climate scenarios that we create by modifying our historic model forcings to show how changes in  
35 evapotranspiration and precipitation can affect groundwater level frequencies.

## 36 2 Study site and data availability

37 Located in West Dorset in the south-west of England the river Frome drains a rural catchment with an area approximately 414 km<sup>2</sup>  
38 (Figure 1). The catchment elevation varies from over 200 m above sea level (a.s.l.) in the north-west to sea level in the south-east.  
39 The topography is very flat with a mean slope of 3.9 % and a mean height of approximately 111 m a.s.l.. The climate can be defined  
40 as oceanic with mild winters and warm summers (Dorset County Council, 2009). Howden (2006) characterised the Frome as highly



1 groundwater-dominated. During the summer months, discharge of the Frome typically is very low, hardly reaching 5 m<sup>3</sup>/s (Brunner  
2 et al., 2010). The geology is predominated by the Cretaceous Chalk outcrop which underlays around 65 % of the catchment. The  
3 headwaters of the Frome include outcrops of the Upper Greensand, often overlain by the rather impermeable Zig-Zag Chalk  
4 (Howden, 2006). The middle reaches of the Frome traverse the Cretaceous Chalk outcrop followed by Palaeogene strata in the lower  
5 reaches, eventually draining into Poole Harbour. The major aquifer Chalk appears mainly unconfined. However, in the lower reaches  
6 it is overlain by Palaeogene strata, resulting in confined aquifer conditions. The region around the Frome catchment is known for  
7 the highest density of solution features in the UK (Edmonds, 1983) which can be mainly observed in the interfluvium between the  
8 Frome and Piddle (Adams et al., 2003). Loams over chalk, shallow silts, deep loamy, sandy and shallow clays constitute the primary  
9 types of soils occurring in the study area (Brunner et al., 2010). The soils of the upper parts of the catchment are mainly shallow  
10 and well drained (NRA, 1995). In the middle and lower reaches the soils are becoming more sandy and acidic due to waterlogged  
11 conditions caused by either groundwater or winter flooding (Brunner et al., 2010; NRA, 1995). Due to its geological setting, the  
12 area is prone to groundwater flooding. It has occurred several times at different locations, for example in Maiden Newton during  
13 winter 2000/2001 (Environment Agency, 2012) and in Winterbourne Abbas during summer 2012 (Bennett, 2013).

14

15 **Figure 1: Overview on the Frome catchment**16 **3 Methodology**

17 In order to consider karstic process behaviour in our simulations we use the process-based karst model VarKarst introduced by  
18 Hartmann et al. (2013b). VarKarst includes the karstic heterogeneity and the complex behaviour of karst processes using distribution  
19 functions that represent the variability of soil, epikarst and groundwater and was applied successfully at different karst regions over  
20 Europe (Hartmann et al., 2013a, 2014b, 2016). We use a simple linear relationship that takes into account effective porosities and  
21 base level of the groundwater wells (see Eq. 1) to enable the model to simulate groundwater levels based on the groundwater storage  
22 in VarKarst. Finally, a newly developed percentile approach is used to transfer simulated groundwater level time series into  
23 groundwater level frequency distributions to compare to observed behaviour at a number of monitored wells.

24 **3.1 The model**

25 The VarKarst model operates on a daily time step. Similar to other karst models, it distinguishes between three subroutines  
26 representing the soil system, the epikarst system and the groundwater system but it also includes their spatial variability, which is  
27 expressed by distribution functions that are applied to a set of  $N=15$  model compartments (Figure 2). Pareto functions as distribution  
28 functions have shown to perform best in previous work (Hartmann et al., 2013a, 2013b), as well as the number of 15 model  
29 compartments (Hartmann et al., 2012). Including the spatial variability of subsurface properties in this manner, the VarKarst model  
30 can be seen as a hybrid or semi-distributed model. All relevant equations and model parameters are provided in Table 2 and Table  
31 3, respectively. For a detailed description of VarKarst see Hartmann et al. (2013b).

32

33

34 **Figure 2: The VarKarst model structure**

35

36 The model was driven by two input time series (Precipitation and PET), and the 13 variable model parameters (see Table 3) were  
37 calibrated and evaluated by four observed time series (discharge and the three boreholes, see subsection 3.3). Similar to Kuczera  
38 and Mroczkowski (1998) we use a simple linear homogeneous relationship which translates the groundwater storage [mm] into a  
groundwater level [m a.s.l.]:



$$h_{GW}(t) = \frac{V_{GW,i}(t)}{1000 * p_{GW}} + \Delta h \quad (1)$$

2

3 The related parameters are  $h_{gw}$  [m] and  $p_{gw}$  [-].  $h_{gw}$  is the difference of the base of the contributing groundwater storage (that is  
4 simulated by the model) and the base of the well that is used for calibration and evaluation.  $p_{gw}$  represents the average porosity of  
5 the rock that is intersected by the well.

6

7

**Table 2: Model routines, variables and equations solved in the VarKarst model**

8

### 9 3.2 Data availability

10 The daily discharge data for gauge East Stoke was obtained from the Centre for Ecology & Hydrology (CEH, <http://nrfa.ceh.ac.uk/>  
11 ) and dates back to the 1960s. The borehole data was provided by the Environment Agency (EA) and obtained via the University of  
12 Bristol. The total data used for modelling in this study can be seen in Table 1. The three boreholes (Ashton Farm, Ridgeway and  
13 Black House) comprised high resolution raw data which had been collected at a 15-minute interval. For further analysis, the data  
14 was aggregated to daily time averages. The potential evapotranspiration has a strong annual cycle. Since most recent data from years  
15 2009-2012 was missing, representative PET-years were calculated on the basis of the last fifty years. Climate projections were  
16 obtained from the UK Climate Projections User Interface (UKCP09 UI, <http://ukclimateprojections-ui.metoffice.gov.uk/> ). For more  
17 information about the UKCP see Murphy et al. (2010).

### 18 3.3 Model calibration and evaluation

19 The Kling-Gupta Efficiency (KGE) is used as a performance measure to calibrate against the discharge and the three boreholes. The  
20 KGE is a result of a decomposition of the NSE (and MSE), emphasizing the importance of the different components of the criterion  
21 (Gupta et al., 2009). We use the Shuffled Complex Evolution Method (SCEM) for our calibration. This method explores the  
22 parameter space using a Monte Carlo Markov Chain and searches for posterior distributions of the model parameters (Vrugt et al.,  
23 2003), including the regions with optimum performance. In addition, the posterior parameter distributions derived from SCEM  
24 provide information about the identifiability of the parameters. The more they differ from a uniform final posterior distribution the  
25 higher the identifiability of a model parameter. Parameter ranges were chosen following previous experience with the VarKarst  
26 model (Hartmann et al., 2013a, 2013b, 2014b, 2016). Besides the quantitative measure of efficiency, a split sample test (Klemeš,  
27 1986) was carried out. Our data covered precipitation, evapotranspiration, discharge and groundwater levels from 2000 to the end  
28 of 2012. We calibrated the model on the period 2008-2012 and used the period 2003-2007 for validation. We chose this reversed  
29 order to be able including the information of 3 boreholes that was only available for 2008-2012. Three years were used as warm-  
30 up, respectively. During calibration, the most appropriate of the  $N=15$  groundwater compartments to represent each groundwater  
31 well was found by choosing the compartment with the best correlation to the groundwater dynamics of the well. This procedure was  
32 repeated for each well and each Monte Carlo run and finally provides the three model compartment numbers that produce the best  
33 simulations of groundwater levels at the three operation wells and the best catchment discharge according to our selected weighting  
34 scheme. During calibration we used a weighting scheme which was found by trial and error. Discharge and the borehole at Ashton  
35 Farm were both weighted as one third as Ashton farm is located in the lower parts within the catchment while the other two boreholes  
36 were located at higher elevation at the catchment's edge and weighted one sixth each. In order to explore to contribution of the  
37 different observed discharge and groundwater time series during the calibration, we use SCEM to derive the posterior parameter  
38 distributions using (1) the final weighting scheme, (2) only discharge, (3) only Ashton farm, and (4) only the other two boreholes



1 (equally weighted). Posterior parameter distributions are plotted as cumulative distributions. Deviations of the posterior distribution  
2 (diagonal) indicate a sensitive parameter. The more parameters that show sensitivity, the more information is contained in the  
3 selected calibration scheme.

4

### 5 3.4 The percentile approach

6 Even though the VarKarst model includes spatial variability of system properties by its distribution functions, its semi-distributed  
7 structure does not allow for an explicit consideration of the locations of ground water wells. Its model structure allowed for an  
8 acceptable and stable simulation of groundwater level time series of the three wells (see subsection 4.1) but for groundwater  
9 management, frequency distributions of groundwater levels, calculated over the time scale of interest, are commonly preferred. For  
10 that reason we introduced a groundwater level percentile based approach. Other than Westerberg et al. (2016) that transferred  
11 discharge time series into signatures derived from flow duration curves, we calibrate directly with the discharge and groundwater  
12 time series in order to evaluate the performance of our approach for selected time periods (see evaluation below). Similar to the  
13 calculation of standardised precipitation or groundwater indices (e.g., Bloomfield and Marchant, 2013; Lloyd-Hughes and Saunders,  
14 2002) we create cumulative frequency distributions of observed groundwater levels and the simulated groundwater levels from the  
15 previously evaluated model. Now, the exceedance probability or percentile for a selected observed groundwater level (for instance,  
16 the groundwater level above which groundwater flooding can be expected) can be used to define the corresponding simulated  
17 groundwater level and the number of days exceeding or falling below the chosen groundwater level can directly be extracted from  
18 the frequency distributions (Figure 3). Note that this procedure is performed after the model is calibrated and validated as described  
19 in the previous subsection.

20

21 **Figure 3: schematic description of the percentile approach**

22

23 As the approach is meant to be applied in combination with climate change scenarios, we perform an evaluation on multiple time  
24 scales and flow percentiles. We assess the 5<sup>th</sup>, 10<sup>th</sup>, 25<sup>th</sup>, 50<sup>th</sup>, 75<sup>th</sup>, 90<sup>th</sup> and 95<sup>th</sup> percentiles on temporal resolutions of years, seasons,  
25 months, weeks and days. The deviation between modelled and observed number of exceedance days of these different percentiles  
26 is quantified by the **mean absolute deviation (MAD)** between simulated exceedances and observed exceedances:

27

$$28 \quad MAD_p = \text{mean} \left( \text{abs} \left( \sum obs_{i,x} - \sum sim_{i,x} \right) \right)_p \quad [d] \quad (2)$$

29 Where  $x$  stands for the time scale (years, months, weeks, days) and  $p$  is the respective percentile. To better compare the deviation  
30 for different percentiles we normalize the MAD to a **percentage of mean absolute deviation (PAD)** with the total number of days of  
31 the chosen time scale:

32

$$33 \quad PAD_p = \frac{MAD_p}{dp_x} * 100 \quad [\%] \quad (3)$$

34

35 where  $dp_x$  is a normalizing constant standing for total the number of days of the respective time scale and percentile. For example,  
36 if we take the time scale *months* and the 75<sup>th</sup> percentile of exceedances we got a  $dp_x$  of  $(100-75) \% \times (365.25 / 12)$  days. To evaluate  
37 the prediction performance of the approach, percentiles are calculated based on the calibration period and the applied on the  
38 validation period similar to the split sample test in subsection 3.3. That way we are able to evaluate our model over different  
39 thresholds and in terms of temporal resolution.



### 1 3.5 Establishment of simple climate scenarios and assessment of groundwater level frequency distributions

2 Given the model performance assessment above, we then use our approach to assess future changes of groundwater level frequencies  
3 at our study site. We derive projections of future precipitation and potential evapotranspiration by manipulating our observed  
4 ‘baseline’ climate data. We extract distributional samples of percentage changes of precipitation and evaporation from the UK  
5 probabilistic projections of climate change over land (UKCP09) for (1) a low emission scenario and (2) a high emission scenario  
6 for the time period of 2070-2099. This enables us to capture, in a pragmatic and computationally efficient approach, for the two  
7 emission scenarios the general range of changes for the most pertinent variables that we think will most impact changes to monthly-  
8 seasonal GW responses. We focus on projected median delta values for change in mean temperature (°C) and precipitation (%) as  
9 well as the respective 25<sup>th</sup> and 75<sup>th</sup> percentile from the probabilistic projections and apply them on our input data. For our model  
10 input we transfer projected temperatures into evapotranspiration via the Thornthwaite equation (Thornthwaite, 1948). In this way,  
11 we obtain 3 x 3 projections (3x precipitation and 3x evapotranspiration) for each of the emission scenarios that also address the  
12 uncertainty associated with the projections. The resulting simulations will provide an estimate of possible future changes of  
13 groundwater level frequencies for the two emission scenarios including an assessment of their uncertainty.

## 14 4 Results

### 15 4.1 Model calibration and evaluation

16 Table 3 shows the optimised parameter values as well as the model performance. The simulation of the discharge shows KGE values  
17 of 0.73 and 0.58 in the calibration and validation period, respectively. The borehole simulations show high KGE values and only  
18 slight deteriorations in the validation period. The parameters are located well within their pre-defined ranges. Mean soil storage  
19  $V_{\text{mean,S}}$  and mean epikarst storage  $V_{\text{mean,E}}$  are 2015.6 mm and 1011.7 mm, respectively. The porosity parameter at Ashton Farm is  
20 the highest, followed by the borehole at Black House. Ridgeway shows the smallest porosity value. For Ashton Farm and Blackhouse  
21 the calibration chose the groundwater storage compartment 7, for Ridgeway it chose the compartment number 8.

22 Figure 4 plots the observations against simulations for the calibration and validation period. Modelled discharge generally matches  
23 the seasonal behaviour of the observations. However, some low-flow peaks are not depicted well in the simulation. When looking  
24 at the groundwater levels, the simulation of Ashton Farm appears to be most adequate. However, there are considerable periods  
25 when differences from the observations can be found for all wells. Simulations at Ridgeway and Black House show moderate  
26 performance in capturing peak groundwater levels. Notably the simulation at Black House is slightly better in the validation period.  
27 The cumulative parameter distributions derived by SCEM indicate that the model parameters were well identifiable when we use  
28 all available data (Figure 5), while some parameters remain hardly identifiable when only parts of the available data were used for  
29 calibration. For instance, non-identifiable groundwater porosity and base level parameters if only discharge was used for calibration.

30

31 **Figure 4: Modelled discharge [m<sup>3</sup>/s] of the Frome at East Stoke and groundwater levels [m a.s.l.] at the boreholes Ashton**  
32 **Farm, Ridgeway and Black House**

33

34 **Figure 5: Cumulative parameter distributions (blue) of all model parameters; strong deviation from the 1:1 (dark grey)**  
35 **indicate good identifiability**



## 1 4.2 The percentile approach

2 When simulated peak values of groundwater levels are compared to the observations, we find a rather moderate agreement. Using  
3 the percentile approach we find different thresholds to exceed our selected groundwater level percentiles. This is elaborated for 90<sup>th</sup>  
4 percentile of simulated and observed groundwater levels of Ashton farm (Figure 6).

5

6 **Figure 6: Illustration of the percentile approach. Time series of the observed (grey dots) and modelled (green line)**  
7 **groundwater level at Ashton Farm. The dotted lines represent the respective 90th percentile**

8

9 Table 4 shows the mean observed and modelled exceedances of all selected thresholds (the 5<sup>th</sup>, 10<sup>th</sup>, 25<sup>th</sup>, 50<sup>th</sup>, 75<sup>th</sup>, 90<sup>th</sup>, and 95<sup>th</sup>  
10 percentiles) at all temporal resolutions in the validation period. By comparing matches in the number days of exceedance we evaluate  
11 our model at different percentiles and time scales. The left value is the mean absolute deviation (MAD) and the right value is the  
12 percentage of absolute deviation (PAD). We can see that the higher the percentile the larger is the deviation between observed and  
13 modelled exceedances. The same is true for the PAD when moving from lower to higher temporal resolutions. The MAD gets lower  
14 the higher the temporal resolution is.

15

16 **Table 4: Deviations of simulated to observed exceedances of different percentiles in the validation period (borehole:**  
17 **Ashton Farm). The left value is the mean absolute deviation MAD [d], the right value is the deviation percentage PAD [%]**

18

## 19 4.3 Impact of simulated climate changes on groundwater level distributions

20 The results of applying the two climate projections to the model can be found at Table 5 and in Figure 7. Both emission scenarios  
21 (low & high) lead to an increased modelled actual evapotranspiration and to decreased discharge simulations. In addition, both  
22 emission scenarios show a substantial reduction in exceedances of high percentiles. We also find that the standard error of the  
23 exceedances and non-exceedances of high emission scenario tends to be higher than the standard error of the low emission scenario.

24

25 **Figure 7: Mean (manipulated) input (mm/a), mean modelled output (mm/a) and mean (non-)exceeded percentiles**  
26 **(number/a) in the reference period and both scenarios (borehole: Ashton Farm; future period: 2070-2099). The circles**  
27 **indicate the spread among the 9 realisations for each of the two scenarios**

28

29 **Table 5: Model output and (non-)exceedances of percentiles in the reference period and the two scenarios (borehole:**  
30 **Ashton Farm, time period 2070-2099)**

## 31 5 Discussion

### 32 5.1 Reliability of the simulations

33 The low decrease in model performance during the validation period for the discharge and groundwater time series indicates  
34 acceptable robustness of the calibrated parameters, which is corroborated by their generally mainly high identifiability derived by  
35 SCEM for the final calibration scheme the used all 4 available observed discharge and ground water level time series. Using the  
36 different weighting schemes we also see that only the combined calibration with all 4 time series allowed for identifying all model  
37 parameters, while using the discharge or the groundwater observations alone would have produced posterior distributions that  
38 indicate low sensitivity of some of the model parameters. A look at the parameter values reveals an adequate reflection of the reality.





1 However,  $V_{mean,S}$  and  $V_{mean,E}$  are quite high considering that initial ranges for these parameters were 0-250/0-500 mm (Hartmann et  
2 al., 2013a, 2013c). As previous studies took place in fairly dry catchments, the ranges were extended substantially to deal with the  
3 wetter climate in southern England. A high  $a_{SE}$  indicates a high variability of soil and epikarst thicknesses favouring lateral karstic  
4 flow concentration (Ford and Williams, 2007). Butler et al. (2012) notes that the unsaturated zone of the Chalk is highly variable,  
5 ranging from almost zero near the rivers to over 100 m in interfluvies.

6 Additionally, the mean epikarst storage coefficient  $K_{mean,E}$  is quite low, indicating fast water transport from the epikarst to the  
7 groundwater storage which is in accordance to other studies (e.g., Aquilina et al., 2006). The value of parameter  $a_{fsep}$  indicates that  
8 a significant part of the recharge is diffuse. A moderately high conduit storage coefficient  $K_C$  and a high  $a_{CW}$  indicate that there is a  
9 significant contribution of slow pathways by the matrix system. This is in accordance with the findings of Jones and Cooper (1998)  
10 as well as Reeves (1979) who reported 30 % and 10-20 % of the recharge occurring through (macro-) fissures in Chalk catchments,  
11 respectively. Although groundwater flow in the chalk is dominated by the matrix, given antecedent wet conditions, fracture flow  
12 can increase significantly (Butler et al., 2012; Ireson and Butler, 2011; Lee et al., 2006). Overall, split-sample test, parameter  
13 identifiability analysis, realistic values of parameters and plausible simulation results provide strong indication for a reliable model  
14 functioning.

## 15 **5.2 Performance of the percentile approach**

16 Based on the idea of the standardised precipitation or groundwater indices (Bloomfield and Marchant, 2013; Lloyd-Hughes and  
17 Saunders, 2002) our new percentile approach permits to improve the performance of the model to reflect observed groundwater  
18 level exceedances. It yields acceptable performance for years to days up to the 90<sup>th</sup> percentile. A reduction of precision with the  
19 time scale is obvious but in an acceptable order of magnitude when the validation period is considered. Although deviations are  
20 considerable both in the calibration and validation period, they are stable demonstrating certain robustness but also the limitations  
21 of our approach. Although the variable model structure of the VarKarst model was shown to provide more realistic results than  
22 commonly used lumped models (Hartmann et al., 2013b) it still simplifies a karst system's natural complexity. This is obvious in  
23 the simulated time series at Ashton Farm and Black House indicate, which also an over-estimation of high levels and under-  
24 estimation of low levels. The reason for this behaviour might be due to the modelling assumption of a constant vertical porosity,  
25 despite the knowledge that there can be a strongly non-linear relation between chalk transmissivity and depth. Several studies  
26 acknowledge that hydraulic conductivity in the Chalk follows a non-linear decreasing trend with depth (Allen et al., 1997; Butler et  
27 al., 2009; Wheeler et al., 2007). This is mainly attributed to the decrease of fractures because of the increasing overburden and  
28 absence of water level fluctuations (Butler et al., 2012; Williams et al., 2006). Hydraulic conductivities in the Chalk can span several  
29 orders of magnitude (Butler et al., 2009) and are particularly enhanced at the zone of water table fluctuations (Williams et al., 2006).  
30 In addition, cross-flows occurring in the aquifer can lead to complicated system responses in the Chalk (Butler et al., 2009). For the  
31 sake of a parsimonious model structure, these characteristics were omitted in this study but their future consideration could help to  
32 improve the simulations if information about the depth profile of permeability is available. Such decrease of performance was also  
33 found for standardised indices that use probability distributions instead of a simulation model (Van Lanen et al., 2016; Núñez et al.,  
34 2014; Vicente-Serrano et al., 2012). To improve the approach's reliability for higher groundwater level percentiles, a model  
35 calibration that is more focussed on the high groundwater level percentiles may be a promising direction. A consideration of the  
36 time spans above the 90<sup>th</sup> percentile will allow for a better simulation quality. However, longer time series than available for this  
37 study would be needed for a proper evaluation of this idea.

## 38 **5.3 Applicability and transferability of our approach**

39 We prepared two scenarios by manipulating our input data using probabilistic projections of annual changes of precipitation and  
40 potential evaporation at 2070-2099 for a low and a high emission scenario. This might neglect some of the changes on climate





1 patterns predicted by climate projections but it is based on local and real meteorological values of the reference period therefore  
2 avoiding problems that arise when historic and climate projection data show pronounced mismatches during their overlapping  
3 periods. Our results revealed that both scenarios lead to less exceedances over higher percentiles and more non-exceedances of  
4 lower percentiles indicating a higher risk of groundwater drought at our study site. However, one problem that arises from our  
5 approach is that we do not consider changes in the seasonal patterns of our input variable, for example the increase of winter  
6 precipitation. If this increase was considered the results would probably yield more exceedances of higher percentiles, as for instance  
7 found by Jimenez-Martinez et al. (2015). Although quite simplistic our results are qualitatively in accordance with previous studies  
8 indicating increased occurrence of droughts in the UK (Burke et al., 2010; Prudhomme et al., 2014). The risk of drought occurrences  
9 might increase depending on the magnitude of change in evapotranspiration. However, more research and the application of more  
10 elaborated scenarios is necessary to completely understand the consequences of the change in groundwater frequency patterns in  
11 the UK chalk regions.

12 As the VarKarst model is a process-based model that includes the relevant characteristics of karst systems over range of climatic  
13 settings (Hartmann et al., 2013b) our approach can to some extent be used to assess future changes of groundwater level distributions  
14 and also be applied in other regions. This may bring some advantage concerning approaches that used transfer functions (Jimenez-  
15 Martinez et al., 2015) or regression models (Adams et al., 2010) for estimating groundwater levels, if enough data for model  
16 calibration and evaluation is available.

17 As has been noted by Cobby et al. (2009), the likelihood and depth of groundwater inundations is one of the major challenges for  
18 future research of groundwater flooding. Since it is a lumped approach it may provide, after Butler et al. (2012), "a good indication  
19 of the likelihood of groundwater flooding, but do[es] not indicate where the flooding will take place". A spatial determination of  
20 the groundwater table as in Upton and Jackson (2011) would be possible but only in catchments where the borehole network is  
21 extensive. Thereby, the possibility to model several boreholes with one single calibration, due to compartment structure in VarKarst,  
22 might be also an advantage. Butler et al. (2012) noted that the parameterization of the unsaturated zone is a major difficulty in the  
23 Chalk. Since this study struggles also with the porosity, future work should take a closer look at this subject.

## 24 **6 Conclusions**

25 We used an existing process-based lumped karst model to simulate groundwater levels in a chalk catchment in South England.  
26 Groundwater levels were simulated by translating the modelled groundwater storage into groundwater levels with a simple linear  
27 relationship. To evaluate our approach we analysed the agreement of observed and simulated groundwater level exceedances for  
28 different percentiles. Finally, a simple scenario analysis was undertaken to investigate the potential future changes of groundwater  
29 level frequencies that affect the risk of groundwater flooding as well as the risk of groundwater droughts. The model performance  
30 for discharge and the groundwater levels was satisfying showing the general adequacy of the model to simulate groundwater levels  
31 in the chalk. It also revealed shortcomings concerning higher groundwater levels. This was corroborated by the percentile approach  
32 that showed a robust performance up to the 90<sup>th</sup> percentile. A scenario analysis using UKCP projections on expected regional climate  
33 changes showed that expected changes may lead to an increased occurrence of low groundwater levels due to increasing actual  
34 evaporation. In order to obtain more reliable results we recommend collecting more data about the hydrogeological properties of  
35 our study site to improve the structure of our model regarding the porosity and the unsaturated zone. In addition, longer time series  
36 and an adapted calibration approach which, in particular, emphasizes on the >90<sup>th</sup> percentiles of groundwater levels could  
37 significantly improve our simulations. In addition we propose to apply the method on other catchments to test the transferability of  
38 our approach and to quantify the variability of climate change impacts over a wide range of Chalk catchments across the UK.

39

## 40 **Acknowledgements**



- 1 This publications contains Environment Agency information © Environment Agency and database right. Thanks to Dr Jens Lange
- 2 and Dr Sophie Bachmair, University of Freiburg, for their valuable advice. Support for GC, JF and NH was provided by NERC
- 3 MaRIUS: Managing the Risks, Impacts and Uncertainties of droughts and water Scarcity, grant number NE/L010399/1.
- 4



1 **7 References**

- 2 Adams, B., Peach, D. W. D. and Bloomfield, J. P. J.: The LOCAR hydrogeological infrastructure for the Frome/Piddle catchment,  
3 Br. Geol. Surv., 2003.
- 4 Adams, B., Bloomfield, J. P., Gallagher, A. J., Jackson, C. R., Rutter, H. K. and Williams, A. T.: An early warning system for  
5 groundwater flooding in the Chalk, Q. J. Eng. Geol. Hydrogeol., 43(2), 185–193, doi:10.1144/1470-9236/09-026, 2010.
- 6 Allen, D. J., Brewerton, L. J., Coleby, L. M., Gibbs, B. R., Lewis, M. A., MacDonald, A. M., Wagstaff, S. J. and Williams, A. T.:  
7 The physical properties of major aquifers in England and Wales, edited by D. J. Allen, J. P. Bloomfield, and V. K. Robinson, 1997.
- 8 Aquilina, L., Ladouche, B. and Dörfliker, N.: Water storage and transfer in the epikarst of karstic systems during high flow periods,  
9 J. Hydrol., 327(3), 472–485, 2006.
- 10 Bakalowicz, M.: Karst groundwater: a challenge for new resources, Hydrogeol. J., 13, 148–160, 2005.
- 11 Bennett, C.: South Winterbourne Flood Investigation, , (July), 2013.
- 12 Beven, K. J.: A manifesto for the equifinality thesis, J. Hydrol., 320(1–2), 18–36, 2006.
- 13 Birk, S., Liedl, R. and Sauter, M.: Karst Spring Responses Examined by Process-Based Modeling, Groundwater, 44(6), 832–836,  
14 2006.
- 15 Bloomfield, J. P. and Marchant, B. P.: Analysis of groundwater drought building on the standardised precipitation index approach,  
16 Hydrol. Earth Syst. Sci., 17(12), 4769–4787, doi:10.5194/hess-17-4769-2013, 2013.
- 17 Brunner, P., Dennis, I. and Girvan, J.: River Frome Geomorphological Assessment and Rehabilitation Plan, , (October), 2010.
- 18 Burke, E. J., Perry, R. H. J. and Brown, S. J.: An extreme value analysis of UK drought and projections of change in the future, J.  
19 Hydrol., 388(1–2), 131–143, doi:10.1016/j.jhydrol.2010.04.035, 2010.
- 20 Butler, A. P., Mathias, S. A. and Gallagher, A. J.: Analysis of flow processes in fractured chalk under pumped and ambient  
21 conditions ( UK ), , 1849–1858, doi:10.1007/s10040-009-0477-4, 2009.
- 22 Butler, a. P., Hughes, a. G., Jackson, C. R., Ireson, a. M., Parker, S. J., Wheater, H. S. and Peach, D. W.: Advances in modelling  
23 groundwater behaviour in Chalk catchments, Geol. Soc. London, Spec. Publ., 364(1), 113–127, doi:10.1144/SP364.9, 2012.
- 24 Cobby, D., Morris, S., Parkes, A. and Robinson, V.: Groundwater flood risk management: advances towards meeting the  
25 requirements of the EU floods directive, J. Flood Risk Manag., 2(2), 111–119, doi:10.1111/j.1753-318X.2009.01025.x, 2009.
- 26 Dorset County Council: A Local Climate Impacts Profile for Dorset, 2009.
- 27 Edmonds, C. N.: Towards the prediction of subsidence risk upon the Chalk outcrop, Q. J. Eng. Geol. Hydrogeol., 16(4), 261–266,  
28 doi:10.1144/GSL.QJEG.1983.016.04.03, 1983.
- 29 Environment Agency: Frome and Piddle Catchment Flood Management Plan, 2012.
- 30 Fitzpatrick, C. M.: The hydrogeology of bromate contamination in the Hertfordshire Chalk: double-porosity effects on catchment-  
31 scale evolution, phdthesis, University College London., 2011.
- 32 Fleury, P., Ladouche, B., Conroux, Y., Jourde, H. and Dörfliker, N.: Modelling the hydrologic functions of a karst aquifer under  
33 active water management--the Lez spring, J. Hydrol., 365(3), 235–243, 2009.
- 34 Ford, D. and Williams, P. D.: Karst hydrogeology and geomorphology, book, John Wiley & Sons. 578 pages., 2007.
- 35 Ford, D. C. and Williams, P. W.: Karst Hydrogeology and Geomorphology, John Wiley & Sons., 2013.
- 36 Geyer, T., Birk, S., Liedl, R. and Sauter, M.: Quantification of temporal distribution of recharge in karst systems from spring  
37 hydrographs, J. Hydrol., 348, 452–463, 2008.
- 38 Goldscheider, N. and Drew, D.: Methods in Karst Hydrogeology, edited by I. A. of Hydrogeologists, Taylor & Francis Group,  
39 Leiden, NL., 2007.
- 40 Gupta, H. V., Kling, H., Yilmaz, K. K. and Martinez, G. F.: Decomposition of the mean squared error and NSE performance criteria:  
41 Implications for improving hydrological modelling, J. Hydrol., 377(1), 80–91, 2009.



- 1 Hartmann, A., Lange, J., Weiler, M., Arbel, Y. and Greenbaum, N.: A new approach to model the spatial and temporal variability  
2 of recharge to karst aquifers, *Hydrol. Earth Syst. Sci.*, 16(7), 2219–2231, 2012.
- 3 Hartmann, A., Weiler, M., Wagener, T., Lange, J., Kralik, M., Humer, F., Mized, N., Rimmer, A., Barberá, J. A., Andreo, B.,  
4 Butscher, C. and Huggenberger, P.: Process-based karst modelling to relate hydrodynamic and hydrochemical characteristics to  
5 system properties, *Hydrol. Earth Syst. Sci.*, 17(8), 3305–3321, doi:10.5194/hess-17-3305-2013, 2013a.
- 6 Hartmann, A., Barberá, J. A., Lange, J., Andreo, B. and Weiler, M.: Progress in the hydrologic simulation of time variant recharge  
7 areas of karst systems – Exemplified at a karst spring in Southern Spain, *Adv. Water Resour.*, 54, 149–160,  
8 doi:10.1016/j.advwatres.2013.01.010, 2013b.
- 9 Hartmann, A., Wagener, T., Rimmer, A., Lange, J., Brielmann, H. and Weiler, M.: Testing the realism of model structures to identify  
10 karst system processes using water quality and quantity signatures, *Water Resour. Res.*, 49(6), 3345–3358, 2013c.
- 11 Hartmann, A., Goldscheider, N., Wagener, T., Lange, J. and Weiler, M.: Karst water resources in a changing world: Review of  
12 hydrological modeling approaches, *Rev. Geophys.*, 52(3), 218–242, doi:10.1002/2013rg000443, 2014a.
- 13 Hartmann, A., Mudarra, M., Andreo, B., Marín, A., Wagener, T. and Lange, J.: Modeling spatiotemporal impacts of hydroclimatic  
14 extremes on groundwater recharge at a Mediterranean karst aquifer, *Water Resour. Res.*, 50(8), 6507–6521, 2014b.
- 15 Hartmann, A., Kobler, J., Kralik, M., Dirnböck, T., Humer, F. and Weiler, M.: Model-aided quantification of dissolved carbon and  
16 nitrogen release after windthrow disturbance in an Austrian karst system, *Biogeosciences*, 13(1), 159–174, doi:10.5194/bg-13-159-  
17 2016, 2016.
- 18 Hill, M. E., Stewart, M. T. and Martin, A.: Evaluation of the MODFLOW-2005 conduit flow process, *Ground Water*, 48(4), 549–  
19 559, doi:10.1111/j.1745-6584.2009.00673.x, 2010.
- 20 Howden, N. J. K.: Hydrogeological controls on surface/groundwater interactions in a lowland permeable chalk catchment:  
21 implications for water quality and numerical modelling, phdthesis, Imperial College London (University of London), 2006.
- 22 Ireson, A. M. and Butler, A. P.: Controls on preferential recharge to Chalk aquifers, *J. Hydrol.*, 398(1), 109–123, 2011.
- 23 Jackson, C. R., Meister, R. and Prudhomme, C.: Modelling the effects of climate change and its uncertainty on UK Chalk  
24 groundwater resources from an ensemble of global climate model projections, *J. Hydrol.*, 399(1–2), 12–28,  
25 doi:10.1016/j.jhydrol.2010.12.028, 2011.
- 26 Jackson, C. R., Bloomfield, J. P. and Mackay, J. D.: Evidence for changes in historic and future groundwater levels in the UK, *Prog.*  
27 *Phys. Geogr.*, 39(1), 49–67, 2015.
- 28 Jenkins, G. J., Perry, M. C. and Prior, M. J.: The climate of the United Kingdom and recent trends, BOOK, Met Office Hadley  
29 Centre, Exeter, UK. [online] Available from: [http://www.ukcip.org.uk/wp-content/PDFs/UKCP09\\_Trends.pdf](http://www.ukcip.org.uk/wp-content/PDFs/UKCP09_Trends.pdf), 2008.
- 30 Jimenez-Martinez, J., Smith, M. and Pope, D.: Prediction of groundwater induced flooding in a chalk aquifer for future climate  
31 change scenarios, *Hydrol. Process.*, n/a--n/a, doi:10.1002/hyp.10619, 2015.
- 32 Jones, H. K. and Cooper, J. D.: Water transport through the unsaturated zone of the Middle Chalk: a case study from Fleam Dyke  
33 lysimeter, *Geol. Soc. London, Spec. Publ.*, 130(1), 117–128, doi:10.1144/GSL.SP.1998.130.01.11, 1998.
- 34 Jukić, D. and Denić-Jukić, V.: Groundwater balance estimation in karst by using a conceptual rainfall--runoff model, *J. Hydrol.*,  
35 373(3), 302–315, 2009.
- 36 Klemeš, V.: Operational testing of hydrological simulation models, *Hydrol. Sci. J.*, 31(1), 13–24, doi:10.1080/0262668609491024,  
37 1986.
- 38 Kuczera, G. and Mroczkowski, M.: Assessment of hydrologic parameter uncertainty and the worth of multiresponse data, *Water*  
39 *Resour. Res.*, 34(6), 1481–1489, 1998.
- 40 Ladouche, B., Marechal, J. C. and Dorfliger, N.: Semi-distributed lumped model of a karst system under active management, *J.*  
41 *Hydrol.*, 509, 215–230, doi:10.1016/j.jhydrol.2013.11.017, 2014.
- 42 Van Lanen, H., Laaha, G., Kingston, D. G., Gauster, T., Ionita, M., Vidal, J.-P., Vlnas, R., Tallaksen, L. M., Stahl, K., Hannaford,

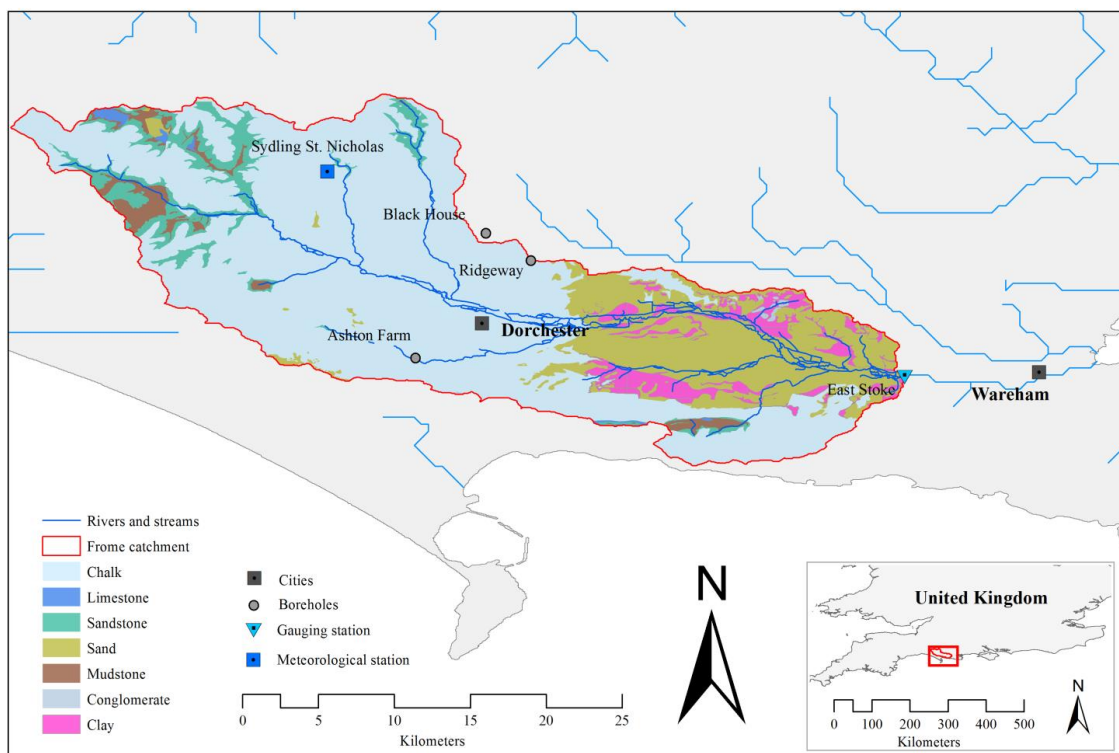


- 1 J., Delus, C., Fendekova, M., Mediero, L., Prudhomme, C., Rets, E., Romanowicz, R. J., Gailliez, S., Wong, W. K., Adler, M.-J.,
- 2 Blauhut, V., Caillouet, L., Chelcea, S., Frolova, N., Gudmundsson, L., Hanel, M., Haslinger, K., Kireeva, M., Osuch, M., Sauquet,
- 3 E., Stage, J. H. and Van Loon, A. F.: Hydrology needed to manage droughts: the 2015 European case, *Hydrol. Process.*, n/a-n/a,
- 4 doi:10.1002/hyp.10838, 2016.
- 5 Lee, L. J. E., Lawrence, D. S. L. and Price, M.: Analysis of water-level response to rainfall and implications for recharge pathways
- 6 in the Chalk aquifer, SE England, *J. Hydrol.*, 330(3), 604–620, 2006.
- 7 Lloyd, J. W.: *The Hydrogeology of the Chalk in North-West Europe*, edited by R. A. Downing, M. Price, and G. P. Jones, pp. 220–
- 8 249, Clarendon Press, Oxford., 1993.
- 9 Lloyd-Hughes, B. and Saunders, M. A.: A drought climatology for Europe, *Int. J. Climatol.*, 22(13), 1571–1592,
- 10 doi:10.1002/joc.846, 2002.
- 11 Macdonald, D., Dixon, A., Newell, A. and Hallaways, A.: Groundwater flooding within an urbanised flood plain, *J. Flood Risk*
- 12 *Manag.*, 5(1), 68–80, 2012.
- 13 Macdonald, D. D. M. J., Bloomfield, J. P. P., Hughes, a. G. G., MacDonald, a. M. M., Adams, B. and McKenzie, a. a.: Improving
- 14 the understanding of the risk from groundwater flooding in the UK, FLOODrisk 2008, Eur. Conf. Flood Risk Manag. Oxford, UK,
- 15 30 Sept - 2 Oct 2008. Netherlands, ~(1), 10 [online] Available from: <http://nora.nerc.ac.uk/7760/>, 2008.
- 16 Maloszewski, P., Stichler, W., Zuber, A. and Rank, D.: Identifying the flow systems in a karstic-fissured-porous aquifer, the
- 17 Schneealpe, Austria, by modelling of environmental <sup>18</sup>O and <sup>3</sup>H isotopes, *J. Hydrol.*, 256(1), 48–59, doi:10.1016/S0022-
- 18 1694(01)00526-1, 2002.
- 19 Maurice, L. D., Atkinson, T. C., Barker, J. A., Bloomfield, J. P., Farrant, A. R. and Williams, A. T.: Karstic behaviour of
- 20 groundwater in the English Chalk, *J. Hydrol.*, 330(1), 63–70, 2006.
- 21 Maurice, L. D., Atkinson, T. C., Barker, J. A., Williams, A. T. and Gallagher, A. J.: The nature and distribution of flowing features
- 22 in a weakly karstified porous limestone aquifer, *J. Hydrol.*, 438–439, 3–15, doi:10.1016/j.jhydrol.2011.11.050, 2012.
- 23 Murphy, J., Sexton, D., Jenkins, G., Boorman, P., Booth, B., Brown, K., Clark, R., Collins, M., Harris, G., Kendon, L., Office, M.,
- 24 Centre, H., Betts, A. R., Brown, S., Hinton, T., Howard, T., McDonald, R., Mccarthy, M., Stephens, A., Atmospheric, B., Centre,
- 25 D., Wallace, C., Centre, N. O., Warren, R., Anglia, E. and Wilby, R.: UK Climate Projections science report : Climate change
- 26 projections, , (December), 2010.
- 27 NRA: *The Frome & Piddle Management Plan - Consultation Report*, 1995.
- 28 Núñez, J., Rivera, D., Oyarzún, R. and Arumí, J. L.: On the use of Standardized Drought Indices under decadal climate variability:
- 29 Critical assessment and drought policy implications, *J. Hydrol.*, 517, 458–470, doi:10.1016/j.jhydrol.2014.05.038, 2014.
- 30 Oehlmann, S., Geyer, T., Licha, T. and Sauter, M.: Reduction of the ambiguity of karst aquifer modeling through pattern matching
- 31 of groundwater flow and transport, *Hydrol. Earth Syst. Sci.*, 16, 11593, doi:10.5194/hess-19-893-2015, 2014.
- 32 Perrin, C., Michel, C. and Andréassian, V.: Improvement of a parsimonious model for streamflow simulation, *J. Hydrol.*, 279, 275–
- 33 289, 2003.
- 34 Prudhomme, C., Giuntoli, I., Robinson, E. L., Clark, D. B., Arnell, N. W., Dankers, R., Fekete, B. M., Franssen, W., Gerten, D.,
- 35 Gosling, S. N., Hagemann, S., Hannah, D. M., Kim, H., Masaki, Y., Satoh, Y., Stacke, T., Wada, Y. and Wisser, D.: Hydrological
- 36 droughts in the 21st century, hotspots and uncertainties from a global multimodel ensemble experiment., *Proc. Natl. Acad. Sci. U.*
- 37 *S. A.*, 111(9), 3262–7, doi:10.1073/pnas.1222473110, 2014.
- 38 Reeves, M. J.: Recharge and pollution of the English Chalk: some possible mechanisms, *Eng. Geol.*, 14(4), 231–240, 1979.
- 39 Reimann, T., Geyer, T., Shoemaker, W. B., Liedl, R. and Sauter, M.: Effects of dynamically variable saturation and matrix-conduit
- 40 coupling of flow in karst aquifers, *Water Resour. Res.*, 47(11), 1–19, doi:10.1029/2011WR010446, 2011.
- 41 Thornthwaite, C. W.: An Approach toward a Rational Classification of Climate, *Geogr. Rev.*, 38(1), 55, doi:10.2307/210739, 1948.
- 42 Upton, K. A. and Jackson, C. R.: Simulation of the spatio-temporal extent of groundwater flooding using statistical methods of



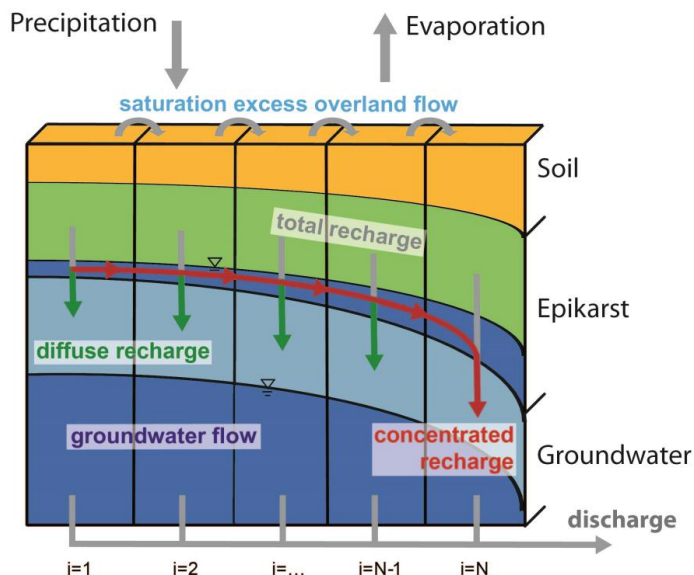
- 1 hydrograph classification and lumped parameter models, *Hydrol. Process.*, 25(12), 1949–1963, 2011.
- 2 Vicente-Serrano, S. M., López-Moreno, J. I., Beguería, S., Lorenzo-Lacruz, J., Azorin-Molina, C. and Morán-Tejeda, E.: Accurate
- 3 Computation of a Streamflow Drought Index, *J. Hydrol. Eng.*, 17(2), 318–332, doi:10.1061/(ASCE)HE.1943-5584.0000433, 2012.
- 4 Vrugt, J. A., Gupta, H. V, Bouten, W. and Sorooshian, S.: A Shuffled Complex Evolution Metropolis algorithm for optimization
- 5 and uncertainty assessment of hydrologic model parameters, *Water Resour. Res.*, 39(8), 1201, doi:10.1029/2002WR001642, 2003.
- 6 Westerberg, I. K., Wagener, T., Coxon, G., McMillan, H. K., Castellarin, A., Montanari, A. and Freer, J.: Uncertainty in hydrological
- 7 signatures for gauged and ungauged catchments, *Water Resour. Res.*, 52, 1847–1865, doi:10.1002/2015WR017635, 2016.
- 8 Wheeler, H. S., Wheeler, H. S., Peach, D. and Binley, A.: Characterising groundwater-dominated lowland catchments : the UK
- 9 Lowland Catchment Research Programme ( LOCAR ) Characterising groundwater-dominated lowland catchments: the UK
- 10 Lowland Catchment Research Programme ( LOCAR ), , 11(1), 108–124, 2007.
- 11 Williams, A., Bloomfield, J., Griffiths, K. and Butler, A.: Characterising the vertical variations in hydraulic conductivity within the
- 12 Chalk aquifer, *J. Hydrol.*, 330(1), 53–62, 2006.
- 13

## 14 8 Figures



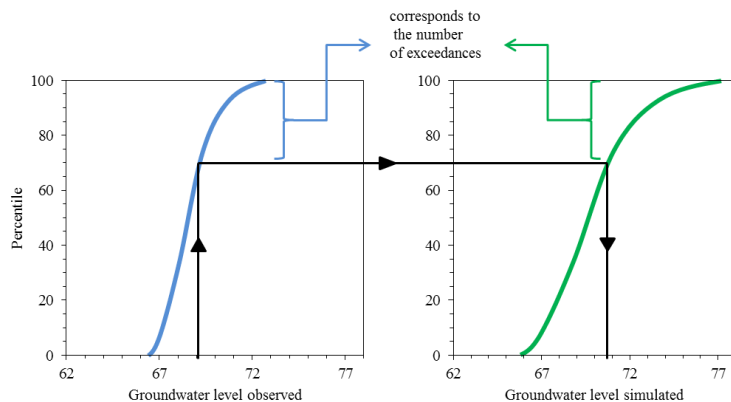
15  
16  
17  
18

Figure 1: Overview on the Frome catchment



1  
 2  
 3

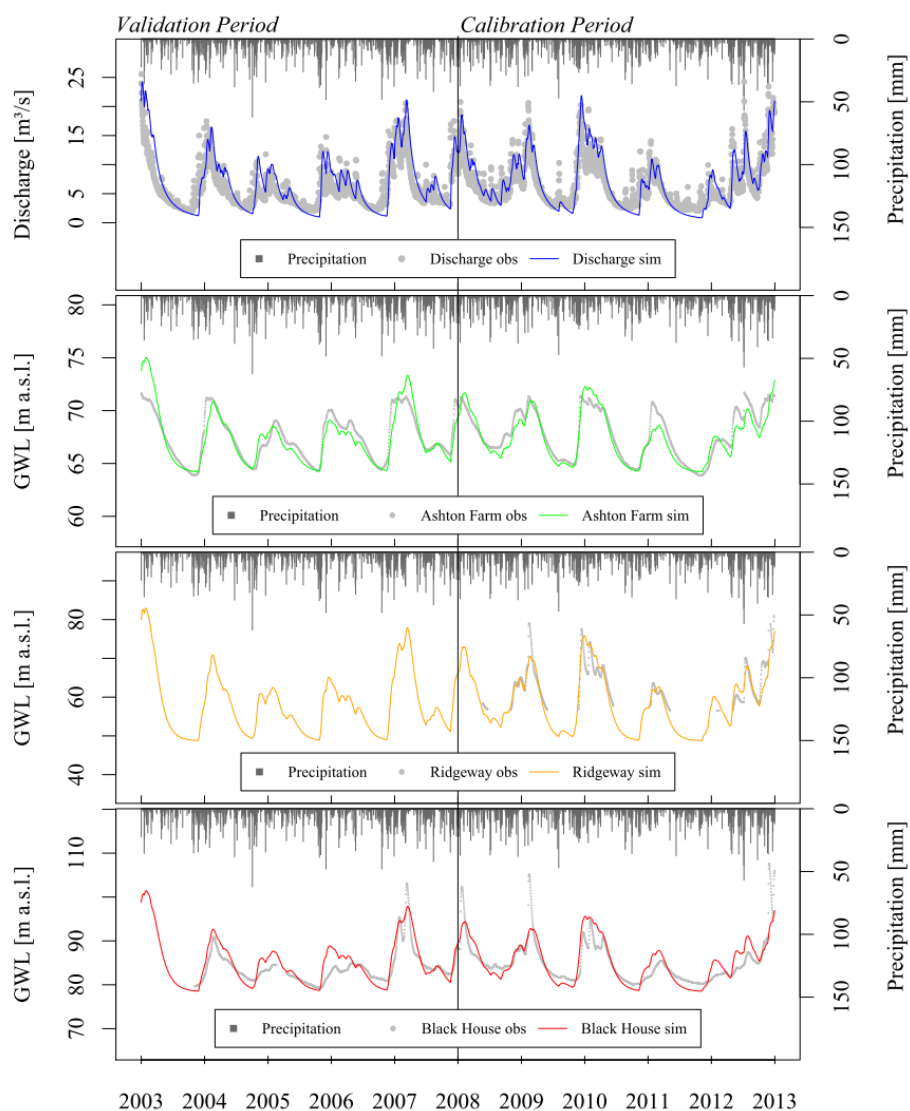
Figure 2: The VarKarst model structure



4  
 5

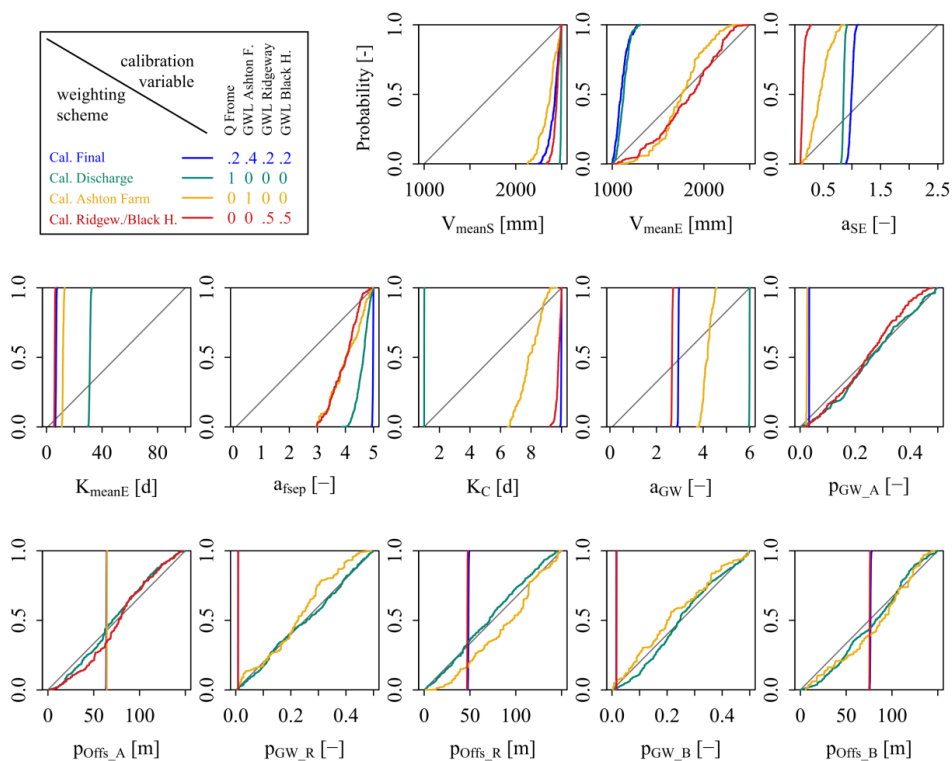
Figure 3: Schematic description of the percentile approach





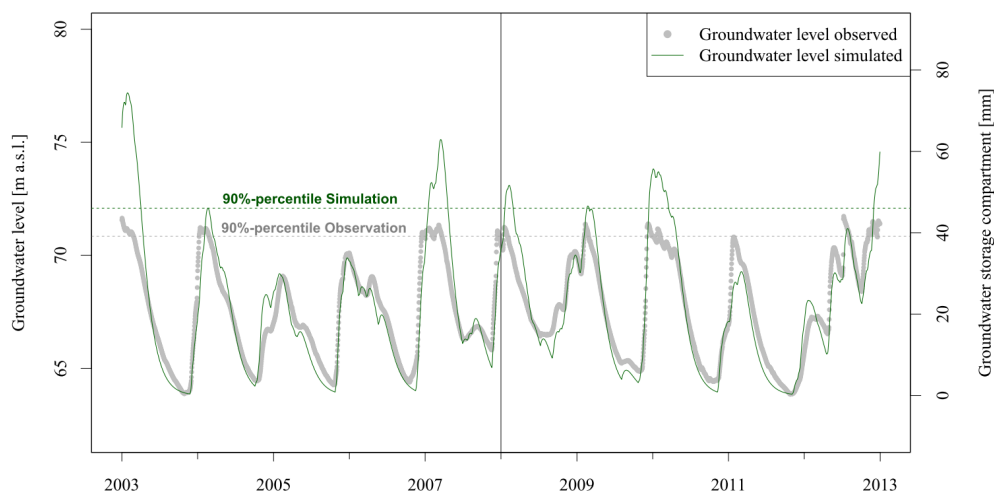
1

2 **Figure 4: Modelled discharge [m<sup>3</sup>/s], and groundwater levels [m a.s.l.] at the boreholes Ashton Farm, Ridgeway and Black House**



1  
 2 **Figure 5: Cumulative parameter distributions (blue) of all model parameters; strong deviation from the 1:1 (dark grey) indicate good**  
 3 **identifiability**

4



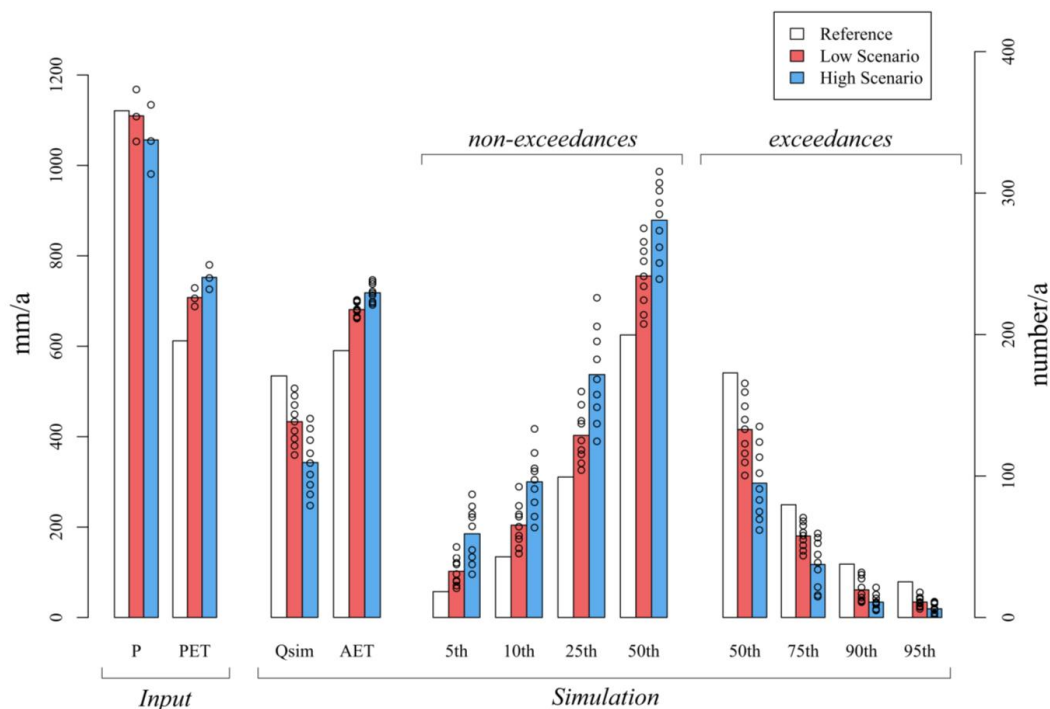
5  
 6 **Figure 6: Illustration of the percentile approach. Time series of the observed (grey dots) and modelled (green line) groundwater level at**  
 7 **Ashton Farm. The dotted lines represent the respective 90th percentile**

8

9



1  
 2  
 3  
 4



5  
 6  
 7  
 8  
 9  
 10

Figure 7: Mean (manipulated) input (mm/a), mean modelled output (mm/a) and mean (non-)exceeded percentiles (number/a) in the reference period and both scenarios (borehole: Ashton Farm; future period: 2070-2099). The circles indicate the spread among the 9 realisations for each of the two scenarios



1 **9 Tables**

2

3 **Table 1: All available data used in the study**

Parameter	Station	Source	Period of time	Resolution	Unit
Precipitation	Sydling St. Nicolas (44006)	CEH	01.01.2000-31.12.2012	daily	mm d <sup>-1</sup>
Discharge	East Stoke (44001)	CEH	01.01.2000-31.12.2012	daily	m <sup>3</sup> s <sup>-1</sup>
Pot. Evapotranspiration	Catchment Cut East Stoke	CEH	01.01.2000-31.12.2008	daily	mm d <sup>-1</sup>
Groundwater Levels	Ashton Farm, Ridgeway, Black House	EA	01.01.2003-31.12.2012	daily	m a.s.l.
Climate Delta values	Grid Box Nr. 1698 (25*25 km)	UKCP	2070-2099	annual	°C, %

4



Table 2: Parameters, descriptions and equations solved in the Varkarst model

Model routine	Variable	Description	Equation	Unit
Soil	$E_{pot,i}(t)$	Actual evapotranspiration	$= E_{pot}(t) \frac{\min[V_{soil,i}(t) + P(t) + Q_{Surface,i}(t), V_{s,i}]}{V_{s,i}}$	mm d <sup>-1</sup>
	$Q_{surf,i+1}(t)$	Surface flow to the next model compartment	$= \max[V_{ep,i}(t) + R_{ep,i}(t) - V_{s,i}, 0]$	mm d <sup>-1</sup>
	$V_{max,s}$	Maximum soil storage capacity	$= V_{mean,s} 2^{\left(\frac{\alpha_{SE}}{\alpha_{SE} + 1}\right)}$	mm
	$V_{s,i}$	Soil storage distribution	$= V_{max,s} \left(\frac{i}{N}\right)^{\alpha_{SE}}$	mm
	$R_{ep,i}(t)$	Recharge to the epikarst	$= \max[V_{soil,i}(t) + P(t) + Q_{Surface,i}(t) - E_{act,i}(t) - V_{s,i}]$	mm d <sup>-1</sup>
Epikarst	$V_{max,E}$	Maximum epikarst storage capacity	$= V_{mean,E} 2^{\left(\frac{\alpha_{SE}}{\alpha_{SE} + 1}\right)}$	mm
	$V_{E,i}$	Epikarst storage distribution	$= V_{max,E} \left(\frac{i}{N}\right)^{\alpha_{SE}}$	mm
	$Q_{ep,i}(t)$	Outflow of the epikarst	$= \frac{\min[V_{ep,i}(t) + R_{ep,i}(t) + Q_{Surface,i}(t) + Q_{Surface,i}(t), V_{E,i}]}{K_{E,i}} \Delta t$	mm d <sup>-1</sup>
	$K_{E,i}$	Epikarst storage coefficient	$= K_{max,E} \left(\frac{N-i+1}{N}\right)^{\alpha_{SE}}$	d
	$R_{diff,i}(t)$	Diffuse recharge	$= f_{c,i} Q_{ep,i}(t)$	mm d <sup>-1</sup>
	$R_{conc,i}(t)$	Concentrated recharge	$= (1 - f_{c,i}) Q_{ep,i}(t)$	mm d <sup>-1</sup>
	$f_{c,i}$	Recharge separation factor	$= \left(\frac{i}{N}\right)^{\alpha_{fcp}}$	-
Groundwater	$Q_{GW,i}(t)$	Groundwater contributions of the matrix	$= \frac{V_{GW,i}(t) + R_{diff,i}(t)}{K_{GW,i}}$	mm d <sup>-1</sup>
	$Q_{GW,N}(t)$	Groundwater contribution of the conduit system	$= \frac{\min[V_{GW,N}(t) + \sum_{i=1}^N R_{conc,i}(t), V_{crit,DF}]}{K_C} \Delta t$	mm d <sup>-1</sup>
	$K_{GW,i}$	Variable groundwater storage coefficient	$= K_C \left(\frac{N-i+1}{N}\right)^{-\alpha_{GW}}$	d
	$Q_{main}(t)$	Discharge	$= \frac{A_{max}}{N} \sum_{i=1}^N Q_{GW,i}(t)$	l s <sup>-1</sup>



1

2 **Table 3: Model parameters, descriptions, ranges and optimised values**

Parameter	Description	Unit	Ranges		Weighting	Optimised Values
			Lower	Upper		
$V_{mean,S}$	Mean soil storage capacity	mm	1000	2500		2015.6
$V_{mean,E}$	Mean epikarst storage capacity	mm	1000	2500		1011.7
$K_{mean,E}$	Epikarst mean storage coefficient	d	0.1	2.5		0.7246
$K_C$	Conduit storage coefficient	d	1	100		38.722
$\alpha_{fsep}$	Recharge separation variability constant	-	0.1	5		1.1864
$\alpha_{GW}$	Groundwater variability constant	-	1	10		5.9966
$\alpha_{SE}$	Soil/epikarst depth variability constant	-	0.1	6		1.8928
$p_{GW,A}$	Ashton Farm groundwater level porosity parameter	-	0.001	0.5		0.0069
$\Delta h_{GW,A}$	Ashton Farm groundwater level offset parameter	m	0	150		64.167
$p_{GW,R}$	Ridgeway groundwater level porosity parameter	-	0.001	0.5		0.0016
$\Delta h_{GW,R}$	Ridgeway groundwater level offset parameter	m	0	150		48.718
$p_{GW,B}$	Black House groundwater level porosity parameter	-	0.001	0.5		0.0032
$\Delta h_{GW,B}$	Black House groundwater level offset parameter	m	0	150		78.448
$KG E_Q$	Model performance for discharge	-	0	1	0.2	0.73/0.58*
$KG E_{GW,A}$	Model performance for groundwater level at Ashton Farm	-	0	1	0.4	0.94/0.80*
$KG E_{GW,R}$	Model performance for groundwater level at Ridgeway	-	0	1	0.2	0.86/ - *
$KG E_{GW,B}$	Model performance for groundwater level at Black House	-	0	1	0.2	0.83/0.74*

\*Calibration/validation.

3

4

5



**Table 4: Deviations of simulated to observed exceedances of different percentiles in the validation period (borehole: Ashton Farm). The left value is the mean absolute deviation MAD [d], the right value is the deviation percentage PAD [%]**

Time period	Percentiles						
	5	10	25	50	75	90	95
<b>5 years</b>	5.00 / 0.29	30.00 / 1.83	38.00 / 2.77	16.00 / 1.75	1.26 / 5.04	19.00 / 10.40	90.00 / 98.56
<b>years</b>	2.60 / 0.75	13.60 / 4.14	14.40 / 5.26	21.20 / 11.61	4.33 / 17.30	19.80 / 54.21	26.00 / 142.37
<b>year-seasons</b>	0.65 / 0.75	4.10 / 4.99	3.60 / 5.26	6.90 / 15.11	6.74 / 26.94	6.45 / 70.64	6.50 / 142.37
<b>months</b>	0.22 / 0.75	1.37 / 4.99	1.20 / 5.26	2.73 / 17.96	7.94 / 31.76	2.58 / 84.87	2.23 / 146.75
<b>weeks</b>	0.05 / 0.74	0.33 / 5.27	0.27 / 5.18	0.61 / 17.36	7.82 / 31.27	0.58 / 83.56	0.54 / 153.10
<b>days</b>	0.01 / 0.75	0.05 / 5.35	0.04 / 5.26	0.09 / 17.96	7.94 / 31.76	0.08 / 84.88	0.08 / 159.91

5

**Table 5: Model output and (non-)exceedances of percentiles in the reference period and the two scenarios (borehole: Ashton Farm, time period 2070-2099)**

Scenario	Qsim	AET	5th	10th	25th	50th	75th	90th	95th
	mm/a	mm/a	non exc/a	non exc/a	non exc/a	exc/a	exc/a	exc/a	exc/a
Reference	534	590	17.6	41.3	95.6	172.9	79.7	37.7	25.2
Low	433	681	31.4	62.8	123.9	132.9	57.6	19.5	10.9
High	343	718	57.0	92.3	165.3	94.9	37.5	10.9	6.1

10